ACS APPLIED MATERIALS & INTERFACES

Research Article

www.acsami.org

Near-Surface Oxidized Sulfur Modifications and Self-Assembly of Thiol-Modified Aptamer on Au Thin Film Substrates Influenced by Piranha Treatment

Joseph P. Thomas, Liyan Zhao, Kejian Ding, Nina F. Heinig, and Kam Tong Leung*

WATLab and Department of Chemistry, University of Waterloo, Waterloo, Ontario, Canada N2L3G1

Supporting Information

ABSTRACT: Self-assembly of thiol-modified oligonucleotides on Au films has great importance for biosensor applications. Prior to the self-assembly, a piranha treatment (PT) is commonly used to clean the Au surface. Here we report that near-surface oxidized sulfur modifications on Au thin films by PT for longer than 60 s have serious effects on the self-assembled monolayer (SAM) formation of thiol-modified single-stranded thrombin binding aptamer (s-TBA), and a PT time of 10−30 s is optimal for s-TBA SAM formation. These results have important implication to SAM formation of biomolecules, especially for the thiol-modified ones where a careful consideration of this key step could significantly enhance the SAM formation and biosensor performance.

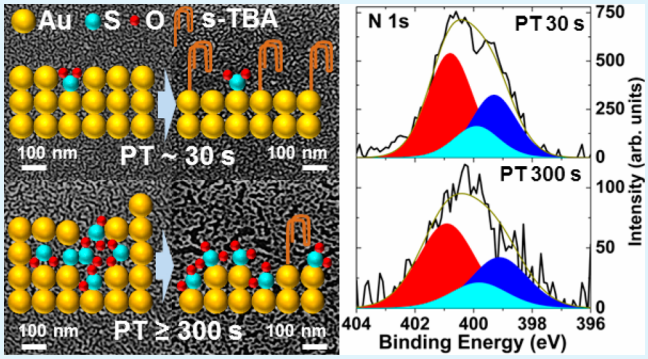

KEYWORDS: *Au thin films, piranha treatment, thrombin binding aptamer, self-assembly, oxidized sulfur modifications*

INTRODUCTION

Advancement in nanobiotechnology promoted the realization of high affinity, highly specific, and stable nanobiosensors with self-assembled monolayers (SAMs) of aptamers, the single-stranded oligonucleotides. At present, SAMs of thiol-modified aptamers on gold films have been used as an important platform for the nanobiosensor fabrication.[1−8] The thrombin binding aptamer (TBA) with a quadruplex structure can specifically bind to thrombin in blood plasma, making TBA one of the most widely used aptamer for the fabrication of aptasensors or nanobiosensors.[1,6−12] Among the diverse substrate materials, Au is a favorite choice for fabricating biosensors mainly because of its biocompatibility and chemical inertness.[2,13−20] TBA sensors have been principally fabricated via the self-assembly of thiol-modified TBA (s-TBA) on Au substrates, where the strong Au−S chemical bond provides the backbone for the sensor platform.[16−22] However, there remain many ambiguities about solvent effects and the mechanism of SAM formation on the substrate surface.

The miniaturization of biosensors and rising cost of Au metal provide powerful incentives for using thinner films for the fabrication of Au-based biosensors. The currently used Au thin films for bio-applications are generally fabricated with a thickness of 15−20 nm.[2] Prior to SAM fabrication on Au films, a surface cleaning step is invariably used. This quintessential step is intended to eliminate organic contaminants on the Au surface. There have been several Au surface cleaning methods, including UV/O_3, aqua regia, reductive annealing, surface polishing, and piranha pretreatments.[19−25] Among these, the surface cleaning using piranha solution (***Caution!*** *It is a strong oxidizer.*) is one of the most popular choices because of the ease of its chemicals availability, preparation, and use.[20−25] It is also known that the piranha treatment (PT) process not only cleans the surface but can also change the surface morphology and oxidize substrate surface.[16,21−28] Although most of the previous reports indicate that they typically use 10−60 min PT to clean the Au surface, there is still no clear validation for the proper amount of PT time that should be employed to produce a good SAM. No due consideration of its effects on surface chemical state and nanostructure modifications, especially for SAM formation of s-TBA on Au surfaces, is available in the literature.

Here we report the formation of an oxidized sulfur layer in the near-surface region that significantly changes the surface morphology and chemical states because of PT on Au thin films. The extent of this oxidized sulfur layer formation depends entirely on the PT time. Furthermore, we have chosen the s-TBA (5′-HS-$(CH_2)_6$-GGTTGGTGTGGTTGG-3′) as a model oligonucleotide to demonstrate the effect of PT time on its SAM formation on Au thin film substrates, which is greatly influenced by the oxidized sulfur layer formation. The present work is the first report establishing the strong influence of PT on s-TBA SAM formation on an Au film surface.

Received: August 7, 2012
Accepted: October 5, 2012
Published: October 5, 2012

 © 2012 American Chemical Society dx.doi.org/10.1021/am301589k | *ACS Appl. Mater. Interfaces* 2012, 4, 5945−5948

EXPERIMENTAL SECTION

Au films with a thickness of 15 nm were fabricated individually on a RCA-cleaned, p-type Si(100) substrate, pre-deposited with a Ti adhesion layer (2.5 nm thick), by using a dual-target magnetron sputtering system (EMS575X) in an Ar atmosphere (after pumping down the chamber to high vacuum of 1×10^{-6} Torr). Unless stated otherwise, s-TBA (5′−HS−$(CH_2)_6$−GGTTGGTGTGGTTGG−3′) and all other chemicals (with the highest available purity) were purchased from Sigma Aldrich and used without further purification. Piranha solution was prepared using 3:1 H_2SO_4 and H_2O_2 (30%) and then used for piranha treatment (PT) of the Au film substrates. PT times of 10, 30, 60, 300, 600, and 1800 s were used to investigate its effects on the Au surface. After PT, the samples were thoroughly washed with Milli-Q water. The as-received s-TBA was initially centrifuged and then mixed with autoclaved Milli-Q water to obtain a concentration of 100 μM and then kept at 4 °C. For SAM formation on Au thin films, 1 μM s-TBA was prepared in 10 mM phosphate-buffered saline (PBS) made of K_2HPO_4 and KH_2PO_4 (with pH 8.0 adjusted by adding KOH). Before immersing the samples into 1 mL of 1 μM s-TBA in 10 mM PBS, 100 mM KCl was added and incubated for 4−6 h to provide sufficient K^+ ions to form quadruplex structures with s-TBA.

Three sets of Au thin film samples were simultaneously prepared, and after the PT, one set was immediately transferred to the XPS system (Thermo-VG Scientific ESCALab 250) equipped with a monochromatic Al Kα source (1486.6 eV), capable of an energy resolution of 0.4−0.5 eV full width at half-maximum (FWHM). XPS spectra were collected and fitted with the Casa-XPS software after appropriate correction with the Shirley background. Peak fittings for the C−C, C−O and C═O C 1s features for the Au films before and after PT were carried out by applying similar FWHM constraints. The peak fittings for the N 1s peaks were performed by employing the FWHM constraints and the appropriate stoichiometric ratios for the −N═, $-NH_2-$, and −NH− components in s-TBA. The second set of samples was used to study the surface morphology by using a field-emission scanning electron microscope (LEO 1530 FESEM). The 1800 s PT almost completely destroyed the Au surface and thus omitted from further studies. Immediately after the PT, the third set of samples was separately immersed for 1 h in the s-TBA solution in order to make the self-assembled monolayers. After SAM formation, the samples were rinsed with Milli-Q water and then dried by blowing N_2 gas before further characterization.

RESULTS AND DISCUSSION

To evaluate in detail the efficacy of PT for contaminant removal, its potential in modifying the surface morphology and chemical states, and its influence on s-TBA SAM formation on PT Au films, high-resolution X-ray photoelectron spectroscopy (XPS) studies have been employed. Comparison between the C 1s peak positions (Figure 1a) and fitted peak areas (Figure 1a, inset) of an Au film without and with PT for 10, 30, 60, 300, and 600 s clearly shows the efficiency of surface cleaning as well as the surface chemical-state modifications. The pristine Au film and Au films after PT exhibit a C−C C 1s peak at 284.7 eV binding energy (BE), except for the 600 s or longer PT Au film with the C−C peak located 0.2 eV higher (at 284.9 eV). The BEs for both the C−O and C═O C 1s peaks are shifted by 0.2 eV or higher for the 300 s or longer PT samples when compared to those with a shorter PT time (286.5 and 288.8 eV) or to the pristine Au film. However, the Au $4f_{7/2}$ peak still remains at 84.0 eV (see Figure S1 in the Supporting Information). The C 1s BE shift found for the Au films with longer PT could be attributed to the PT-induced gold oxide formation.[22−28] It is apparent from the variations of the C−C, C−O, and C═O C 1s peak areas (Figure 1a, inset) that the samples after 300 s PT are more susceptible to immediate

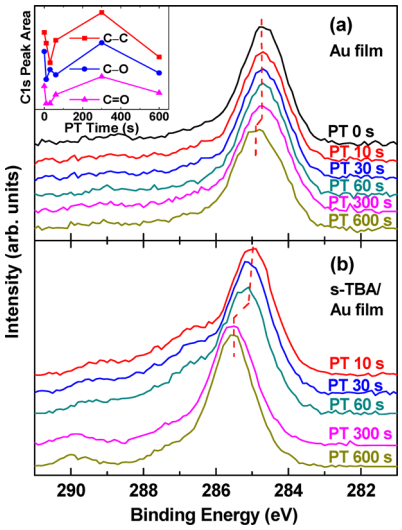

Figure 1. XPS spectra of the C 1s region of (a) Au films before or after piranha treatment (PT) of 10 to 600 s and (b) s-TBA self-assembled monolayers on the corresponding PT Au films. The inset shows the corresponding C 1s peak areas obtained by using Casa XPS peak fitting software.

environmental contamination than those with shorter PT. Prolonged PT (1800 s) could lead to the formation of Au oxide[16] and also etching away the thin films.

The C 1s features for SAMs formed on Au films with PT lie at a higher BE than the corresponding PT Au films without SAMs (Figure 1b). It is interesting to note that the samples with PT, especially those for longer than 60 s, undergo considerably larger changes in their C 1s BE after immersing into s-TBA solution for SAM formation. This is evident from the C 1s spectrum of s-TBA SAMs formed on 300 s or longer PT Au films, with larger C−C or C−H C 1s BE shifts (0.8 eV) than SAMs formed on Au films with a shorter PT (0.3 eV, Figure 1b) with respect to the pristine Au film. This demonstrates that appropriate selection of PT time can significantly affect the SAM formation on Au thin films.

To investigate the sulfur modifications on Au surface due to PT and SAM formation, we measured S 2p spectra for all the samples. No significant S $2p_{3/2}$ peak is observed from the Au films after PT. However, depth-profiling XPS experiment of S 2p region for a 300 s PT Au film reveals a broad peak at 168.5 eV, which is apparent after 10−30 s sputtering (Figure 2a). This result indicates the presence of a near-surface oxidized sulfur (SOx)[29,30] region of about 3−6 nm. In general, for the thiol-modified DNA films, the S $2p_{3/2}$ signal is weak and barely detectable because of the very low relative S concentration and the attenuation by the DNA film.[31] In Figure 2b, a weak peak near 162 eV is found for the s-TBA SAMs formed on the 60 s PT Au film substrate, in addition to the peak at 168.5 eV. The peak near 162 eV suggests the formation of Au−S (thiolate) bonds at the DNA/Au interface.[26,29−31] Surprisingly, we observe a strong broad peak at 168 eV for the SAMs formed on the 300 s PT Au film when compared to that formed on the 60 s PT Au film, which is about 6 eV higher than the Au−S bonds for the SAMs. Thus, the formation of the oxidized sulfur region in Figure 2b is caused by the PT process.

To verify the s-TBA SAM formation on the PT Au films, we monitor the N 1s spectrum of s-TBA SAMs fabricated on Au films with 10, 30, 60, and 300 s PT (Figure 3). The insets in Figure 3 show the corresponding field-emission scanning

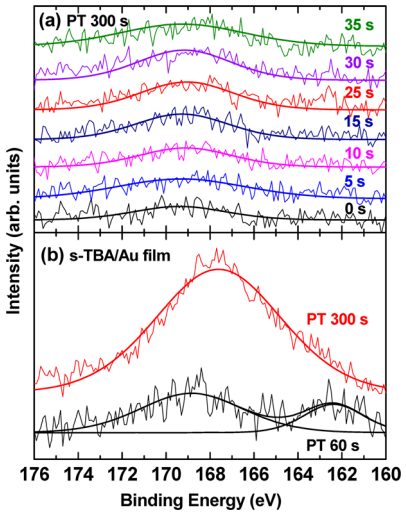

Figure 2. XPS spectra of S 2p region for (a) an Au film with 300 s piranha treatment (PT) after sputtering for 0 to 35 s and (b) s-TBA SAMs on 60 s and 300 s PT Au films.

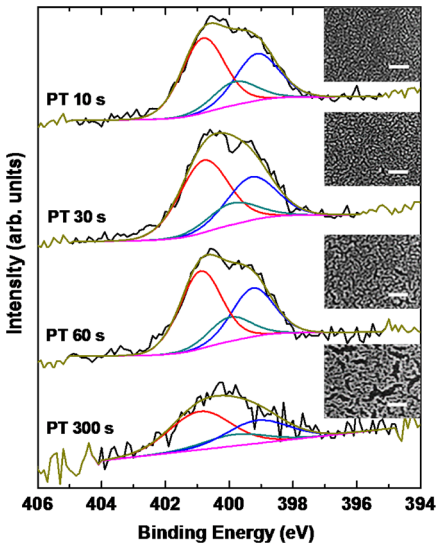

Figure 3. XPS spectra of N 1s region of s-TBA SAMs on Au films after the piranha treatment (PT) for 10, 30, 60, and 300 s. The insets show corresponding SEM images (scale bar 100 nm).

electron microscopy (SEM) images of s-TBA SAMs. The presence of three N 1s peaks with BEs corresponding to −N= at 399.2 eV, $-NH_2$ at 399.9 eV, and −NH− at 400.8 eV confirms the s-TBA SAM formation on substrates. The N 1s peak intensities for s-TBA on the 10 s and 30 s PT Au films show similar SAM formation that is better than those on Au films with 60 s or longer PT (see Figure S2 in the Supporting Information). The packing density of SAMs can also be confirmed by electrochemical methods,[11] and our XPS results are in agreement with the differential pulse voltammetry studies of s-TBA on 10, 30, and 60 s PT Au films (see Figure S3 in the Supporting Information). In addition, no significant surface damage or changes in the Au 4f feature for s-TBA SAMs on Au films with up to 60 s PT are observed. The exposure of the oxidized sulfur region to the s-TBA solution during SAM formation evidently changes the substrate surface morphology (Figure 3, insets). For s-TBA SAMs on Au films with PT longer than 60 s, cracks begin to develop on the samples, though without significant effect on BEs of Au 4f peaks (not shown). By subjecting the samples with a longer PT (above 600 s) to the s-TBA solution, the PT-initiated damage cascade becomes more evident and crack formation on Au thin films accelerates (see Figure S1 in the Supporting Information), causing destruction of the Au films.

We show in Figure 4 a schematic representation of the microstructural modifications on Au films due to PT and s-TBA

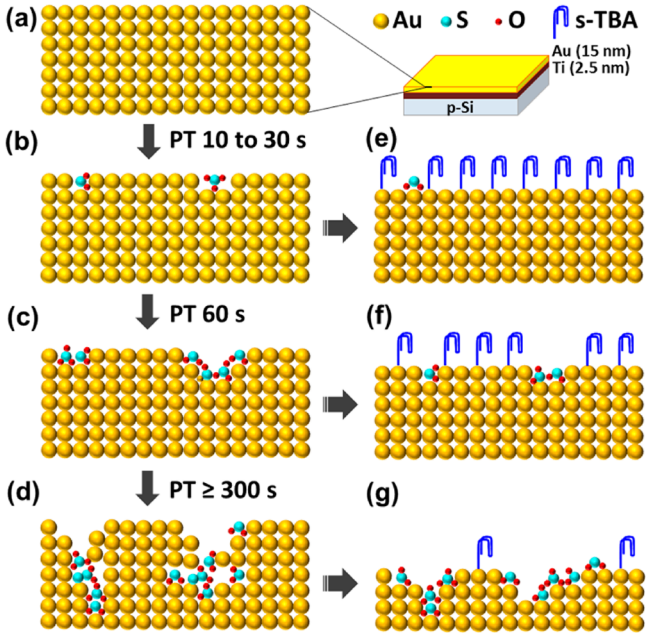

Figure 4. Schematic representation of (a–d) oxidized sulfur formation due to PT (0 to 300 s or above) and of (e–g) s-TBA self-assembly on the corresponding PT Au films.

SAM formation. For simplicity, here we did not depict the elemental carbon dissolution and gold oxide formation by PT. The short PT time of 30 s or less does not induce the formation of a near-surface oxidized sulfur layer on Au film (Figure 4b). However, above 60 s PT (Figure 4c) modifies the surface slightly through the apparent removal of grain boundary gold atoms and initiates binding of a few oxidized sulfur species (SOx) to the grain boundary defect sites. Further PT of 300 s or longer (Figure 4d) enhances the propagation of grain boundary gold atoms removal, migration and bond formation of oxidized sulfur, and formation of a layer of oxidized sulfur in the near-surface region on Au films. During s-TBA SAM formation, the surface morphology of the sample undergone shorter PT (up to 60 s) remains intact (Figure 4e), whereas the s-TBA SAM formation process slightly alters the morphology of 60 s PT sample (Figure 4f). However, significant morphological changes occur for 300 s or above PT samples (Figure 4g). It should be noted that the thiol in TBA could act as an Au surface-cleaner during SAM formation[2] and this self-cleaning effect could remove the top few nanometers of the Au thin films, exposing the near-surface oxidized sulfur region and further enhancing the oxidized sulfur formation. For shorter PT, the self-cleaning effect of s-TBA could effectively clean the surface and form SAMs on Au surface without forming a near-surface oxidized sulfur layer. Longer PT times produced a near-surface oxidized sulfur layer, which we believe propagated through their grain boundary migration and is exposed during SAM formation as a result of the self-cleaning effect of s-TBA.

In addition to the exposed oxidized sulfur region, the formation of oxidized sulfur during s-TBA self-assembly together results in the intense S 2p feature (Figure 2b). It is interesting to note that the exposed oxidized sulfur species appear to be strongly bonded to the Au atoms. This oxidized sulfur layer could not be removed even by the self-cleaning effect of s-TBA, which instead enhances the oxidized sulfur formation and thus further reduced the possible binding sites for s-TBA.

Our results clearly illustrate that PT time of 10−30 s is sufficient for preparing a high-quality Au thin film substrate for good SAM formation. The results also show that PT time of no longer than 60 s would be ideal for removing C contaminants. Contrary to common belief, PT longer than 60 s is not a good practice, because it could, in addition to removing the contaminants, also changes the surface morphology. PT longer than 60 s produces an oxidized sulfur near-surface region in the Au films that saturates the potential binding sites for the thiol group in s-TBA, thereby inhibiting SAM formation. These results suggest the near-surface oxidized sulfur layer formation due to PT and the subsequent self-cleaning effect by the thiol group in s-TBA solution during the SAM formation.

CONCLUSION

In summary, we have found that surface chemical and nanostructure modifications on Au thin films caused by the commonly used piranha cleaning could significantly affect the self-assembly of thiol-modified s-TBA. Substrate cleaning for a shorter PT time ($\leq$30 s) is efficient to clean and to produce s-TBA SAM formation, while PT longer than 60 s induces significant additional modifications to the surface and the near-surface chemical states caused by formation of oxidized sulfur that hinders the self-assembly of s-TBA. The present study therefore provides important insights into the consequences of the piranha cleaning step in fabricating all nanobiosensors and electronic devices based on Au thin films or nanostructures. We believe that the present results will have important implications on the general development of bio-sensor platforms and offer further improvement strategies for their performance.

ASSOCIATED CONTENT

Supporting Information

FESEM images and corresponding XPS spectra of Au $4f_{7/2}$ region of Au films before and after piranha treatment (PT) for 600 s, and after s-TBA SAM formation. XPS spectra of N 1s region of s-TBA SAMs on Au films after 300 and 600 s PT. Differential pulse voltammograms of s-TBA SAMs on Au films after 10, 30, and 60 s PT. This material is available free of charge via the Internet at http://pubs.acs.org/.

AUTHOR INFORMATION

Corresponding Author

*E-mail: tong@uwaterloo.ca.

Notes

The authors declare no competing financial interest.

ACKNOWLEDGMENTS

This work was supported by the Natural Sciences and Engineering Research Council of Canada.

REFERENCES

(1) Xiao, Y.; Lubin, A. A.; Heeger, A. J.; Plaxco, K. W. *Angew. Chem., Int. Ed.* **2005**, *44*, 5456−5459.
(2) Love, J. C.; Estroff, L. A.; Kriebel, J. K.; Nuzzo, R. G.; Whitesides, G. M. *Chem. Rev.* **2005**, *105*, 1103−1169.
(3) Petrovykh, D. Y.; Kimura-Suda, H.; Whitman, L. J.; Tarlov, M. J. *J. Am. Chem. Soc.* **2003**, *125*, 5219−5226.
(4) Cho, H.; Baker, B. R.; Wachsmann-Hogiu, S.; Pagba, C. V.; Laurence, T. A.; Lane, S. M.; Lee, L. P.; Tok, J. B. H. *Nano Lett.* **2008**, *8*, 4386−4390.
(5) Mairal, T.; Ozalp, V. C.; Sanchez, P. L.; Mir, M.; Katakis, I.; O'Sullivan, C. K. *Anal. Bioanal. Chem.* **2008**, *390*, 989−1007.
(6) Huajun, Q.; Yanli, S.; Xirong, H.; Yinbo, Q. *Colloids Surf., B* **2010**, *79*, 304−308.
(7) Balamurugan, S.; Obubuafo, A.; Soper, S. A.; McCarley, R. L.; Spivak, D. A. *Langmuir* **2006**, *22*, 6446−6453.
(8) Radi, A. E.; Sanchez, J. L. A.; Baldrich, E.; O'Sullivan, C. K. *J. Am. Chem. Soc.* **2006**, *128*, 117−124.
(9) Du, Y.; Li, B.; Wei, H.; Wang, Y.; Wang, E. *Anal. Chem.* **2008**, *80*, 5110−5117.
(10) Bock, L. C.; Griffin, L. C.; Latham, J. A.; Vermaas, E. H.; Toole, J. J. *Nature* **1992**, *355*, 564−566.
(11) Lu, Y.; Li, X.; Zhang, L.; Yu, P.; Su, L.; Mao, L. *Anal. Chem.* **2008**, *80*, 1883−1890.
(12) Li, T.; Wang, E.; Dong, S. *Chem. Commun.* **2008**, *31*, 3654−3656.
(13) Opdahl, A.; Petrovykh, D. Y.; Kimura-Suda, H.; Tarlov, M. J.; Whitman, L. J. *Proc. Natl. Acad. Sci.* **2007**, *104*, 9−14.
(14) Saha, K.; Agasti, S. S.; Kim, C.; Li, X.; Rotello, V. M. *Chem. Rev.* **2012**, *112*, 2739−2779.
(15) Tabor, R. F.; Morfa, A. J.; Grieser, F.; Chan, D. Y. C.; Dagastine, R. R. *Langmuir* **2011**, *27*, 6026−6030.
(16) Ron, H.; Rubinstein, I. *Langmuir* **1994**, *10*, 4566−4573.
(17) Sun, Y.; Xu, F.; Zhang, Y.; Shi, Y.; Wenab, Z.; Li, Z. *J. Mater. Chem.* **2011**, *21*, 16675−16685.
(18) Ansar, S. M.; Li, U. X.; Zou, U. S.; Zhang., D. *J. Phys. Chem. Lett.* **2012**, *3*, 560−565.
(19) Herne, T. M.; Tarlov, M. J. *J. Am. Chem. Soc.* **1997**, *119*, 8916−8920.
(20) Hoshiya, N.; Shimoda, M.; Yoshikawa, H.; Yamashita, Y.; Shuto, S.; Arisawa, M. *J. Am. Chem. Soc.* **2010**, *132*, 7270−7272.
(21) Day, B. S.; Fiegland, L. R.; Vint, E. S.; Shen, W.; Morris, J. R.; Norton, M. L. *Langmuir* **2011**, *27*, 12434−12442.
(22) Guo, L. H.; Facci, S.; McLendon, G.; Mosher, R. *Langmuir* **1994**, *10*, 4588−4593.
(23) Kang, J.; Rowntree, P. A. *Langmuir* **2007**, *23*, 509−516.
(24) He, X. P.; Wang, X. W.; Jin, X. P.; Zhou, H.; Shi, X. X.; Chen, G. R.; Long, Y. T. *J. Am. Chem. Soc.* **2011**, *133*, 3649−3657.
(25) Feng, G.; Niu, T.; You, X.; Wan, Z.; Kong, Q.; Bi, S. *Analyst* **2011**, *136*, 5058−5063.
(26) Donavan, K. C.; Arter, J. A.; Pilolli, R.; Cioffi, N.; Weiss, G. A.; Penner, R. M. *Anal. Chem.* **2011**, *83*, 2420−2424.
(27) Juodkazis, K.; Juodkazyte, J.; Jasulaitiene, V.; Lukinskas, A.; Sebeka, B. *Electrochem. Commun.* **2000**, *2*, 503−507.
(28) Cook, K. M.; Ferguson, G. S. *Chem. Commun.* **2011**, *47*, 12550−12552.
(29) Mekhalif, Z.; Riga, J.; Pireaux, J. J.; Delhalle, J. *Langmuir* **1997**, *13*, 2285−2290.
(30) Dietrich, M. P.; Horlacher, T.; Lauriault, P. L. G.; Gross, T.; Lippitz, A.; Min, H.; Wirth, T.; Castelli, R.; Seeberger, P. H.; Unger, W. E. S. *Langmuir* **2011**, *27*, 4808−4815.
(31) Petrovykh, D. Y.; Kimura-Suda, H.; Tarlov, M. J.; Whitman, L. J. *Langmuir* **2004**, *20*, 429−440.